

Hydride, Borohydride, and Dinitrogen Pincer Complexes of Ruthenium

Dmitry G. Gusev,^{*,†} Fedor M. Dolgushin,[‡] and Mikhail Yu. Antipin[‡]

Department of Chemistry, Wilfrid Laurier University, Waterloo, Ontario, Canada N2L 3C5, and X-ray Laboratory, Institute of Organoelement Compounds, Russian Academy of Sciences, 28 Vavilov Street, Moscow B-334, Russia

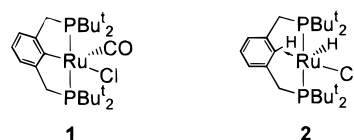
Received May 5, 2000

Reactions of chlorides RuCl(CO)(PCP) (**1**; PCP = [2,6-(CH₂PBu^t)₂C₆H₃][−]) and RuHCl[1,3-(CH₂PBu^t)₂C₆H₄] (**2**) with [Bu₄N]BH₄ in ethanol afforded the hydrides RuH(CO)(PCP) (**3**) and [RuH(PCP)]₂(μ-N₂) (**5a**), respectively. Complex **5a** exists in equilibrium with the dinitrogen species [RuH(N₂)(PCP)](μ-N₂)[RuH(PCP)] (**5b**) and RuH(N₂)(PCP) (**5c**) in solution under N₂. Reaction of **1** and [Bu₄N]BH₄ in ether resulted in formation of the two isomeric borohydride complexes Ru(η²-BH₄)(CO)(PCP) (**4a**) and RuH(CO)[1-BH₃-2,6-(CH₂PBu^t)₂C₆H₃] (**4b**). Single-crystal X-ray structures of **3**, **4b**, and **5a,b** are reported.

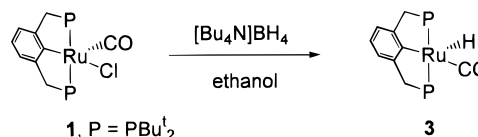
Introduction

Bulky pincer ligands, e.g. [2,6-(CH₂PR₂)₂C₆H₃][−] (R = Prⁱ, Cy, Bu^t), have been studied with late transition metals^{1–3} and show interesting chemistry related to the activation of C–H and other σ-bonds.⁴ Because of the size of the ligands, 16e pincer complexes predominate: examples include cobalt- and nickel-group metals; however, they are scarce outside of the two groups. In group 8, several ruthenium compounds have been obtained from 1,3-(CH₂PPh₂)₂C₆H₄ and RuCl₂(PPh₃)₃, via RuCl(PPh₃)[2,6-(CH₂PR₂)₂C₆H₃].⁵ We have recently reported the preparation and structure of ruthenium complexes

Chart 1



Scheme 1



1 and **2**, incorporating [2,6-(CH₂PBu^t)₂C₆H₃][−] and 1,3-(CH₂PBu^t)₂C₆H₄ ligands (Chart 1).⁶

This paper describes the reactivity of chlorides **1** and **2** toward [BH₄][−] in ethanol and ether, crystal structures of obtained products, and their behavior in solution.

Results

Reaction of 1 with [BH₄][−] in Ethanol. Reaction of RuCl(CO)(PCP) (**1**; PCP = [2,6-(CH₂PBu^t)₂C₆H₃][−]) with tetrabutylammonium borohydride afforded the monohydride RuH(CO)(PCP) (**3**) as a moderately air-sensitive red solid in 85% yield (Scheme 1). The characterization of **3** was accomplished by elemental analysis, NMR and IR spectroscopy, and X-ray diffraction. The square-pyramidal molecular geometry of **3** is illustrated in Figure 1, and selected bond distances and angles are listed in Table 1. We believe that the unsaturated (16e) structure is retained in solution, since the high-field hydride shift δ −27.9 is indicative of a hydride trans to an empty coordination site. Thus, **3** is isostructural with the known five-coordinate complexes RuH(Ph)(CO)(PMeBu^t)₂ (δ_{RuH} −28.6) and RuHCl(CO)-(PPri₃)₂ (δ_{RuH} −24.4).⁷

(6) Gusev, D. G.; Madott, M.; Dolgushin, F. M.; Lyssenko, K. A.; Antipin, M. Yu. *Organometallics* 2000, 19, 1734.

* To whom correspondence should be addressed. E-mail: dgoussev@wlu.ca.

[†] Wilfrid Laurier University.

[‡] Institute of Organoelement Compounds.

(1) (a) Moulton, C. J.; Shaw, B. L. *J. Chem. Soc., Dalton Trans.* 1976, 1020. (b) Nemeh, S.; Jensen, C.; Binamira-Soriaga, E.; Kaska, W. C. *Organometallics* 1983, 2, 1442. (c) Gupta, M.; Hagen, C.; Kaska, W. C.; Flesher, R.; Jensen, C. M. *J. Chem. Soc., Chem. Commun.* 1996, 2083. (d) Vigalok, A.; Uzan, O.; Shimon, L. J. W.; Ben-David, Y.; Martin, J. M. L.; Milstein, D. *J. Am. Chem. Soc.* 1998, 120, 12539.

(2) (a) Cross, R. J.; Kennedy, A. R.; Muir, K. W. *J. Organomet. Chem.* 1995, 487, 227. (b) Cross, R. J.; Kennedy, A. R.; Muir, K. W. *Inorg. Chim. Acta* 1995, 231, 207. (c) Kennedy, A. R.; Cross, R. J.; Muir, K. W. *Inorg. Chim. Acta* 1995, 231, 195.

(3) (a) Ohff, M.; Ohff, A.; van der Boom, M. E.; Milstein, D. *J. Am. Chem. Soc.* 1997, 119, 11687. (b) Rybtchinski, B.; Ben-David, Y.; Milstein, D. *Organometallics* 1997, 16, 3786. (c) Liu, F.; Pak, E. B.; Singh, B.; Jensen, C. M.; Goldman, A. S. *J. Am. Chem. Soc.* 1999, 121, 4086. (d) van der Boom, M. E.; Kraatz, H.-B.; Hassner, L.; Ben-David, Y.; Milstein, D. *Organometallics* 1999, 18, 3873.

(4) (a) A review: Rybtchinski, B.; Milstein, D. *Angew. Chem., Int. Ed.* 1999, 38, 870. (b) Rybtchinski, B.; Vigalok, A.; Ben-David, Y.; Milstein, D. *J. Am. Chem. Soc.* 1996, 118, 12406. (c) Gupta, M.; Hagen, C.; Kaska, W. C.; Cramer, R. E.; Jensen, C. M. *J. Am. Chem. Soc.* 1997, 119, 840. (d) Lee, D. W.; Kaska, W. C.; Jensen, C. M. *Organometallics* 1998, 17, 1. (e) van der Boom, M. E.; Liou, Sh.-Y.; Ben-David, Y.; Shimon, L. J. W.; Milstein, D. *J. Am. Chem. Soc.* 1998, 120, 6531. (f) van der Boom, M. E.; Liou, Sh.-Y.; Ben-David, Y.; Gozin, M.; Milstein, D. *J. Am. Chem. Soc.* 1998, 120, 13415. (g) van der Boom, M. E.; Ben-David, Y.; Milstein, D. *J. Am. Chem. Soc.* 1999, 121, 6552. (h) Rybtchinski, B.; Milstein, D. *J. Am. Chem. Soc.* 1999, 121, 4528. (i) Jensen, C. M. *J. Chem. Soc., Chem. Commun.* 1999, 2443.

(5) (a) Karlen, T.; Dani, P.; Grove, D.; M.; Steenwinkel, P.; van Koten, G. *Organometallics* 1996, 15, 5687. (b) Jia, G.; Lee, H. M.; Xia, H. P.; Williams, I. D. *Organometallics* 1996, 15, 5453. (c) Lee, H. M.; Yao, J.; Jia, G. *Organometallics* 1997, 16, 3927. (d) Jia, G.; Lee, H. M.; Williams, I. D. *J. Organomet. Chem.* 1997, 534, 173.

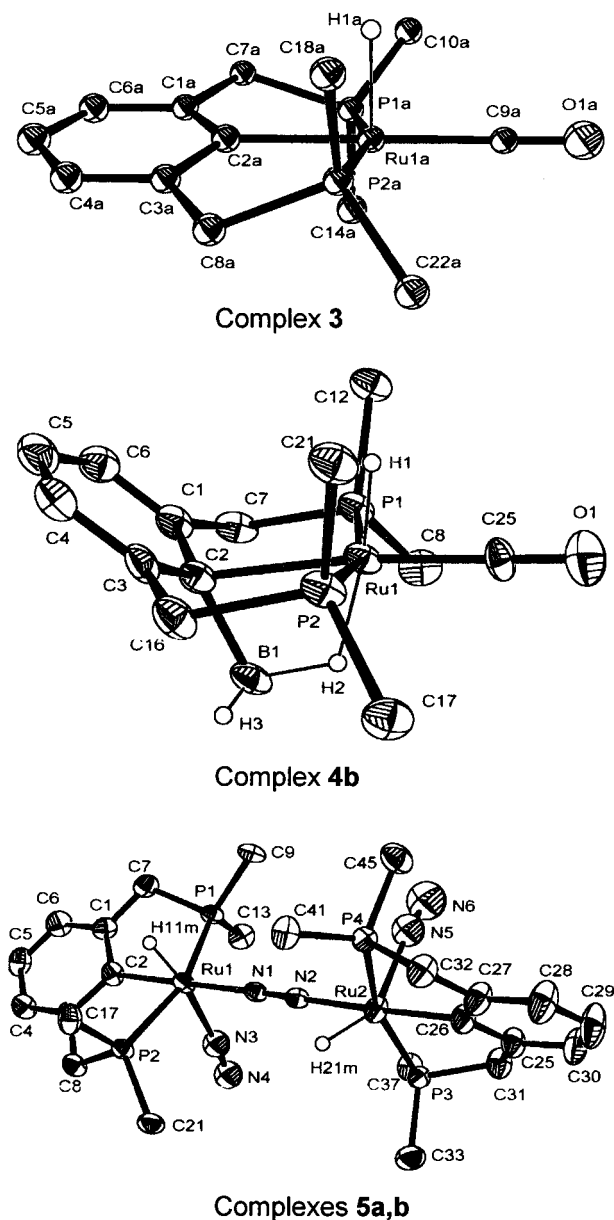


Figure 1. Molecular structures of complexes **3** (one of the two independent molecules shown), **4b**, and **5a,b**. Non-metal hydrogens and methyl groups are omitted for clarity. Thermal ellipsoids are at the 50% probability level.

Reaction of 1 with $[\text{BH}_4]^-$ in Ether. Reactions of 16e metal halides with BH_4^- involve X^-/BH_4^- substitution and intermediate formation of 18e borohydrides.⁸ Thus, $\text{Ru}(\eta^2\text{-BH}_4)(\text{CO})(\text{PCP})$ could be expected from **1** according to Scheme 2, prior to formation of **3**. To avoid alcoholysis, we carried out this reaction in diethyl ether and obtained a yellow air-stable solid. The microanalytical data for the isolated product were in agreement with the anticipated formulation, $\text{Ru}(\text{BH}_4)(\text{CO})(\text{PCP})$ (**4a**). The IR spectrum of **4a** shows two bands in the terminal B–H region at 2444 and 2335 cm^{-1} and two bands in the bridging M–H–B region at 1948 and 1939 cm^{-1} , consistent with the bidentate $\eta^2\text{-BH}_4$ binding mode.⁸ In the ^1H NMR spectrum, **4a** shows a broad

resonance of the two bridging hydrides at -5.4 ppm and another broad feature at δ 4 belonging to the terminal boron hydrides.

A small amount (19%) of another compound was observed by NMR in the isolated product. It could be independently prepared by addition of $\text{H}_3\text{B}\cdot\text{THF}$ to monohydride **3** and characterized as $\text{RuH}(\text{CO})[\text{1-BH}_3\text{-2,6-(CH}_2\text{P}^t\text{Bu}_2)_2\text{C}_6\text{H}_3]$ (**4b**; Scheme 3). The crystal structure of **4b** is shown in Figure 1, and selected bond distances and angles are compiled in Table 1. A slow quantitative formation of **4b** from **4a** was observed in THF (50% isomerization after 2 h).

Reaction of 2 with $[\text{BH}_4]^-$ in Ethanol. Reaction of $\text{RuHCl}[\text{1,3-(CH}_2\text{P}^t\text{Bu}_2)_2\text{C}_6\text{H}_4]$ (**2**) with $[\text{BH}_4]^-$ resulted in high-yield isolation of a dark violet air-sensitive solid formulated as the dimer $[\text{RuH}(\text{PCP})]_2(\mu\text{-N}_2)$ (**5a**; Scheme 4) on the basis of the IR, NMR, X-ray, and microanalytical data. The hydride of **5a** is observed at δ -31.6 , shift consistent with this ligand being trans to an empty coordination site in a square-pyramidal ruthenium fragment. The $^{31}\text{P}\{^1\text{H}\}$ NMR spectrum of **5a** is an AB spin system ($^2J_{\text{PP}} = 259$ Hz) due to the inequivalent trans P^tBu_2 groups of two staggered $[\text{RuH}(\text{PCP})]$ fragments.

The two related dinitrogen complexes **5b,c** are formed from **5a** in solution under nitrogen (Scheme 5). Complex **5b** was detected and characterized by single-crystal X-ray diffraction in a sample of **5a** crystallized under N_2 . The structure in Figure 1 shows a disordered terminal dinitrogen ligand of **5b** with low occupancy of 0.2 N_2 per ruthenium, according to refinement. The third compound **5c** is more soluble than the equilibrium partners **5a,b** and could not be crystallized. The square-pyramidal geometry shown in Scheme 5 is supported by the NMR observations of the hydride triplet at δ -29.73 and single chemical shift in the ^{31}P NMR spectrum.

5c is the dominant species in solution under nitrogen; e.g., a **5c**:**5a** molar ratio of 86:14 was measured in benzene- d_6 (28 mmol of $[\text{Ru}]$, 1 atm of N_2 , 20 $^\circ\text{C}$). In the NMR spectra of this mixture the hydride and phosphorus resonances of both compounds were somewhat broad due to the equilibrium with undetected **5b** (Scheme 5). The **5c**:**5a** ratio changed to 55:45 under vacuum, and the NMR spectra sharpened. A close to initial 89:11 **5c**:**5a** ratio was established when nitrogen was readmitted into the NMR tube.

The bridging N_2 ligand of **5a** is not observed in the IR spectrum of the isolated solid (Nujol mull), which shows a weak hydride stretch at 2160 cm^{-1} , similar to the 2105 and 2130 cm^{-1} Ru–H vibrations in **3** and **4b**. The IR spectrum of **5a–c** recorded in toluene under N_2 showed an intense band at 2088 cm^{-1} assigned to the $\text{N}\equiv\text{N}$ stretching vibration of **5c**.

Reaction of 2 with $[\text{BH}_4]^-$ in Ether. Reaction of **2** with tetrabutylammonium borohydride in Et_2O was attempted; however, the products were unstable and the ^{31}P NMR spectrum of the reaction mixture revealed multiple peaks of decomposition species. Another attempt to prepare a borohydride complex by reacting **5a–c** with $\text{H}_3\text{B}\cdot\text{THF}$ resulted in similar decomposition chemistry that was not pursued further.

Crystal Structures of Complexes 3, 4b, and 5a,b. **Complex 3.** Crystallographic analysis of **3** reveals

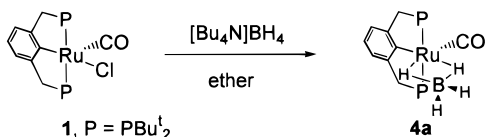
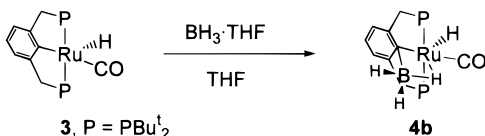
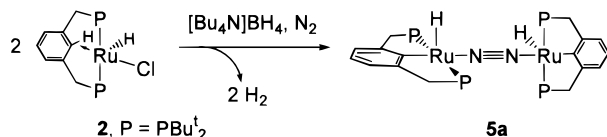
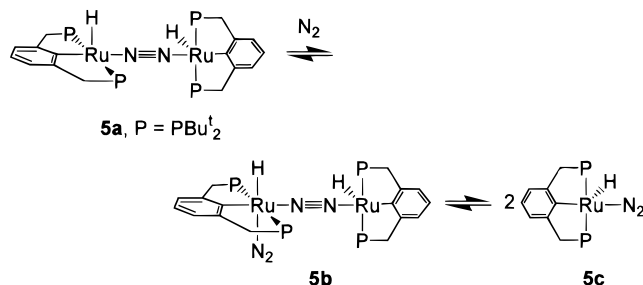
(7) (a) Heyn, R. H.; Macgregor, S. A.; Nadasdi, T. T.; Ogasawara, M.; Eisenstein, O.; Caulton, K. G. *Inorg. Chim. Acta* **1997**, 259, 5. (b) Esteruelas, M. A.; Werner, H. J. *Organomet. Chem.* **1986**, 303, 221.
(8) Marks, T. J.; Kolb, J. R. *Chem. Rev.* **1977**, 77, 263.

Table 1. Selected Bond Distances (Å) and Bond Angles (deg) for Complexes **3**, **4b**, and **5a,b**

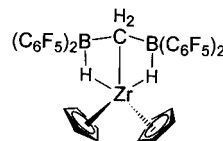
complex 3 ^a		complex 4b		complexes 5a,b	
Ru(1)–C(2)	2.108(4)	Ru(1)–C(2)	2.291(14)	Ru(1)–C(2)	2.080(5)
Ru(1)–C(9)	1.901(4)	Ru(1)–C(25)	1.839(11)	N(1)–N(2)	1.134(6)
Ru(1)–H(1)	1.73(7)	Ru(1)–H(1)	1.34(17)	N(3,5)–N(4,6) ^b	1.13(4)
Ru(1)–P(1)	2.310(1)	Ru(1)–P(1)	2.352(4)	Ru(1)–P(1)	2.333(1)
Ru(1)–P(2)	2.323(1)	Ru(1)–P(2)	2.349(4)	Ru(1)–P(2)	2.330(1)
C(9)–O(1)	1.143(5)	C(25)–O(1)	1.113(15)	Ru(1,2)–N(1,2) ^b	2.038(4)
		C(2)–B(1)	1.63(2)	Ru(1,2)–N(3,5) ^b	2.17(3)
C(2)–Ru(1)–H(1)	90(2)	C(2)–Ru(1)–H(1)	103(6)	C(2)–Ru(1)–N(1)	178.09(14)
C(2)–Ru(1)–C(9)	177.95(15)	C(2)–Ru(1)–C(25)	172.6(6)	C(2)–Ru(1)–N(3)	91.8(8)
C(2)–Ru(1)–P(1)	80.71(12)	C(2)–Ru(1)–P(1)	83.1(3)	C(2)–Ru(1)–P(1)	80.03(13)
C(2)–Ru(1)–P(2)	81.45(13)	C(2)–Ru(1)–P(2)	84.1(3)	C(2)–Ru(1)–P(2)	79.81(13)
C(9)–Ru(1)–P(1)	99.28(11)	C(25)–Ru(1)–P(1)	97.8(5)	N(1)–Ru(1)–P(1)	101.10(10)
C(9)–Ru(1)–P(2)	98.44(11)	C(25)–Ru(1)–P(2)	96.3(5)	N(1)–Ru(1)–P(2)	98.97(10)
C(9)–Ru(1)–H(1)	88(2)	C(25)–Ru(1)–H(1)	85(6)	N(3)–Ru(1)–P(1)	91.7(27)
P(1)–Ru(1)–P(2)	161.99(4)	P(1)–Ru(1)–P(2)	163.01(12)	N(3)–Ru(1)–P(2)	92.1(7)
H(1)–Ru(1)–P(1)	97(2)	H(1)–Ru(1)–P(1)	83(7)	P(1)–Ru(1)–P(2)	159.59(5)
H(1)–Ru(1)–P(2)	83(2)	H(1)–Ru(1)–P(2)	89(7)	Ru(1)–N(1)–N(2)	178.3(3)
		Ru(1)–C(2)–B(1)	71.7(8)	N(1)–Ru(1)–N(3)	89.7(8)
		C(5)–C(2)–B(1)	155.2(7)	Ru(1)–N(3)–N(4)	175(2)
		C(5)–C(2)–Ru(1)	133.2(8)	H(11m)–Ru(1)–N(1)	101(4)

^a Bond lengths and angles have been averaged for the two independent molecules (see the Supporting Information for full data).

^b Averaged bond lengths.

Scheme 2**Scheme 3****Scheme 4****Scheme 5**

square-pyramidal geometry about ruthenium (Figure 1) where the hydride occupies the apical position. The carbonyl is trans to the carbon of the PCP ligand. The two exert a strong mutual trans influence that explains the relatively long Ru(1)–C(9) and Ru(1)–C(2) bonds: 1.901(4) and 2.108(4) Å. In the parent compound **1**, the two atoms are cis, and their bonds to ruthenium are shorter: 1.757(5) and 2.076(4) Å, respectively.⁶ As expected, the C–O bond is longer for the shorter Ru–CO: 1.183(6) Å in **1** vs 1.143(5) in **3**. For some reason,

Chart 2

IR spectroscopy is insensitive to the structural differences, and the carbonyl stretching frequencies are similar in **1** (1909 cm^{-1})⁶ and **3** (1906 cm^{-1}).

Complex 4b. The molecular structure of **4b** in Figure 1 shows an η^2 -coordinated C(2)–B(1)–H(2) borate fragment linked with two metal-bonded phosphorus groups. In total, $[\text{H}_3\text{BAR}]^- = [\text{1-BH}_3\text{-2,6-(CH}_2\text{PBu}_2^t)_2\text{C}_6\text{H}_3]^-$ is an 8-electron donor, and **4b** is formally an 18-electron complex of Ru(II). The C(2)–B(1) distance is 1.63(2) Å that is close to the sum of the atomic radii for these bonding partners, 1.65 Å. The C–B bond length is 1.643 Å in dimesityl borohydride.⁹ The absence of any appreciable C(2)–B(1) bond elongation in **4b** and also the long C(2)–Ru(1) distance of 2.291(14) Å suggest that the side-on (C–B)Ru bonding must be inefficient. Although the C(2)–B(1) bond is removed from the C_6 plane by ca. 24.8° , there is no other distortion in the ring structure, and the aromaticity is apparently not affected by the weak (C–B)Ru interaction.

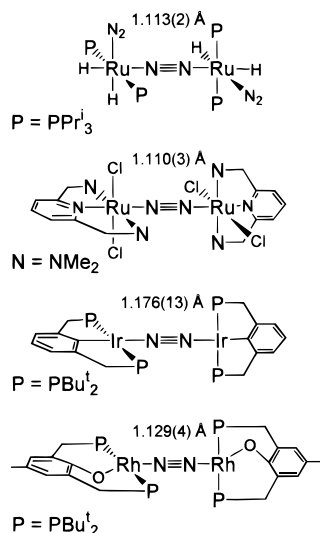
A remotely similar bonding arrangement involving a methylene carbon of $[(\text{C}_6\text{F}_5)_2\text{HB}-\text{CH}_2-\text{BH}(\text{C}_6\text{F}_5)_2]^{2-}$ coordinated to zirconium has been characterized by X-ray analysis.¹⁰ In this structure (Chart 2), both the C–B distance (1.695(7) Å) and B–C–B angle ($149.3(4)^\circ$) are greater than the values expected for the uncoordinated ligand. Stronger (C–B)Zr bonding in this molecule is probably a consequence of the dianionic nature of the ligand, which is coordinated to a d^0 early-transition-metal center.

Complexes 5a,b. The third structure in Figure 1 for complexes **5a,b** can be compared to four related struc-

(9) Hooz, J.; Akiyama, S.; Cedar, F. J.; Bennett, M. J.; Tuggle, R. M. *J. Am. Chem. Soc.* **1974**, *96*, 274.

(10) von H. Spence, R. E.; Parks, D. J.; Piers, W. E.; MacDonald, M.-A.; Zaworotko, M. J.; Rettig, S. J. *Angew. Chem., Int. Ed. Engl.* **1995**, *34*, 1230.

Chart 3



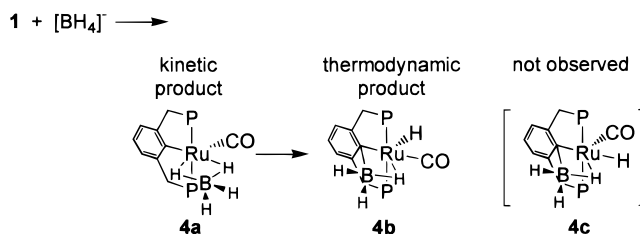
tures of ruthenium,^{11,12} rhodium,^{4e} and iridium^{4d} pincer complexes in Chart 3. The bridging N(1)–N(2) distance of 1.134(6) Å in **5a,b** is within the range of N≡N distances in the four $\mu\text{-N}_2$ species. The metal–nitrogen bonds (trans to the PCP carbon) are similar in **5a,b** and in the iridium complex: 2.038(4) and 2.007(11) Å. The iridium and ruthenium dimers all show the staggered conformation of the metal fragments that minimizes ligand repulsion. The disordered terminal N_2 ligand of **5b** has been refined less accurately; however the N≡N distance (1.13(4) Å) is normal.¹³

Discussion

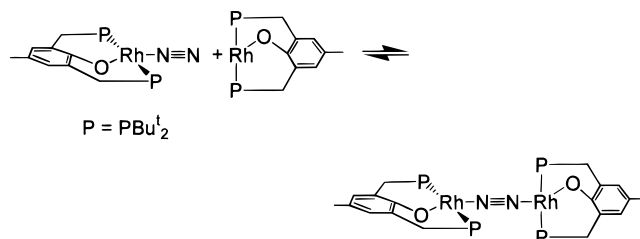
Formation of Complexes 3–5. Ethanolic borohydride “reduction” of transition-metal halides is commonly employed for the preparation of metal hydrides. The intermediacy of $(\text{BH}_4)\text{M}$ species in this reaction is well-known, and such borohydride complexes can be isolated, for example, when the alcoholysis is suppressed by the use of a massive excess of $[\text{BH}_4]^-$.⁸ In a more tractable way, $\eta^2\text{-BH}_4$ species can be prepared in ether using $[\text{Bu}_4\text{N}]\text{BH}_4$, which is sufficiently reactive in this solvent.¹⁴

From the chloride $\text{RuCl}(\text{CO})(\text{PCP})$ (**1**) we obtained the anticipated borohydride $\text{Ru}(\eta^2\text{-BH}_4)(\text{CO})(\text{PCP})$ (**4a**) in diethyl ether and the monohydride $\text{RuH}(\text{CO})(\text{PCP})$ (**3**) in ethanol. An unexpected development in this part of our work was the discovery of isomerization of **4a** into another borohydride compound, $\text{RuH}(\text{CO})[1\text{-BH}_3\text{-2,6-(CH}_2\text{PBu}^t_2)_2\text{C}_6\text{H}_3]$ (**4b**). This reaction appears to be strongly solvent-dependent. It takes several hours in THF but a much longer time in Et_2O , where the isomerization is incomplete in 24 h. Both **4a** and **4b** seem indefinitely stable in less polar benzene. A plausible means of formation of **4b** would involve borane elimination from **4a** as a solvent complex: e.g., $\text{H}_3\text{B}\cdot$

Scheme 6



Scheme 7



THF. Upon this elimination, the monohydride $\text{RuH}(\text{CO})(\text{PCP})$ is formed that should eventually recapture BH_3 to give **4b** according to Scheme 3. We know that when a stronger base NEt_3 (1 equiv) is used, borane is eliminated from **4a** quantitatively and irreversibly, to give $\text{H}_3\text{B}\cdot\text{NEt}_3$ and $\text{RuH}(\text{CO})(\text{PCP})$.

We postulate **4b** to be the thermodynamic product in the reaction of **1** and $[\text{BH}_4]^-$ (Scheme 6). It is, however, unclear what structural feature makes **4b** more favorable than **4a** and why the third possible isomer **4c** is apparently the least stable in this system, since it has not been observed.

The borohydride reduction of $\text{RuHCl}[1,3\text{-(CH}_2\text{PBu}^t_2)_2\text{-C}_6\text{H}_4]$ (**2**) afforded dinitrogen complexes **5a–c** in ethanol under N_2 . By analogy with **4** and **3**, in this reaction we expected intermediate formation of borohydride and hydride species, such as $\text{RuH}(\eta^2\text{-BH}_4)[1,3\text{-(CH}_2\text{PBu}^t_2)_2\text{-C}_6\text{H}_4]$, $\text{RuH}_2[1,3\text{-(CH}_2\text{PBu}^t_2)_2\text{C}_6\text{H}_4]$, or their isomers. We have not isolated these species, which are unstable and tend to eliminate H_2 . In ethanol, they further coordinate N_2 to form **5a–c**, and the least soluble dimer **5a** precipitates from the reaction solution.

A similar mixture of mono- and binuclear rhodium complexes is known, and it has been postulated that a 14e intermediate is involved in the equilibrium between the dinitrogen species, as shown in Scheme 7.^{4e} Our three compounds **5a–c** also exchange nitrogen in solution. The associative mechanism in Scheme 5 does not require formation of 14e $\text{RuH}(\text{PCP})$ from $\text{RuH}(\text{N}_2)(\text{PCP})$ (**5c**), although this cannot be completely ruled out, since terminal dinitrogen is a labile ligand.

Concluding Remarks

In continuation of our research with bulky pincer complexes of ruthenium, we have developed convenient, high-yield synthetic routes to new unsaturated 16e monohydrides **3** and **5a**. Compounds **5a–c** contain dinitrogen ligands and might be precursors of the 14e species $[\text{RuH}(\text{PCP})]$ in solution. As described in this paper, the two borohydride complexes **4a,b** constitute an interesting molecular system, and a computational study might be desirable for better understanding of the structure and bonding.

(11) Abdur-Rashid, K.; Gusev, D. G.; Lough, A. J.; Morris, R. H. *Organometallics* **2000**, *19*, 1652.

(12) Abbenhuis, R. A. T. M.; del Rio, I.; Bergshoeff, M. M.; Boersma, J.; Veldman, N.; Spek, A. L.; van Koten, G. *Inorg. Chem.* **1998**, *37*, 1749.

(13) Hidai, M.; Mizobe, Y. *Chem. Rev.* **1995**, *95*, 1115.

(14) Gusev, D.; Llamazares, A.; Artus, G.; Jacobsen, H.; Berke, H. *Organometallics* **1999**, *18*, 75.

Experimental Section

General Comments. All room-temperature reactions were carried out under nitrogen in a glovebox. When heating was required in the preparation of **3**, the reaction mixture was transferred out of the box, attached to a manifold, and opened under N₂. The reaction vessel was returned into the box for the isolation of the product. Anhydrous deuterated and regular solvents were stored and used in the glovebox. NMR measurements were done on a Varian VXR 200 spectrometer. Throughout this paper, the NMR data are reported with the apparent coupling of observed virtual triplets (vt) denoted as $^{\nu}J$. [Bu₄N]-BH₄ and 1 M H₃B·THF solution were purchased from Aldrich. Complexes **1** and **2** were prepared according to published procedures.⁶

Preparation of RuH(CO)[2,6-(CH₂PBu₂)₂C₆H₃] (3). A suspension containing **1** (1.8 g, 3.22 mmol) and [Bu₄N]BH₄ (0.9 g, 3.50 mmol) in ethanol (30 mL) was stirred for 3 h at room temperature and for a further 2 h at 80 °C. Then it was left overnight at room temperature. The product was isolated by filtration, washed with 3 × 5 mL of ethanol, and dried under vacuum for 3.5 h. Yield: 1.43 g (85%). Anal. Calcd for C₂₅H₄₄OP₂Ru (523.64): C, 57.34; H, 8.47. Found: C, 57.25; H, 8.29. IR (Nujol): ν_{CO} 1906 cm⁻¹, ν_{RuH} 2105 cm⁻¹. ¹H NMR (CD₂Cl₂): δ -27.90 (t, $^2J_{\text{HP}}$ = 18.5 Hz, 1H, Ru H), 1.19, 1.29 (vt, $^{\nu}J$ = 6.5, 6.2 Hz; 36H, CH₃), 3.50, 3.56 (m, overlapped, 4H, CH₂), 6.87 (t, $^3J_{\text{HH}}$ = 7.3 Hz, 1H, C₆H₃), 7.09 (d, 2H, C₆H₃). ³¹P{¹H} NMR (CD₂Cl₂): δ 98.4 (doublet in the hydride-coupled spectrum). ¹³C{¹H} NMR (C₆D₆): δ 29.34, 30.26 (vt, $^{\nu}J$ = 3.1 Hz, CH₃), 34.29 (vt, $^{\nu}J$ = 8.6 Hz, PCH₂), 36.94 (vt, $^{\nu}J$ = 6.6 Hz, PCH₂), 39.15 (vt, $^{\nu}J$ = 10.8 Hz, PCH₂), 120.91 (vt, $^{\nu}J$ = 8.6 Hz, CH, Ar), 124.86 (t, $^4J_{\text{CP}}$ = 1.1 Hz, CH, Ar), 153.88 (vt, $^{\nu}J$ = 11.5 Hz, C, Ar), 187.97 (t, $^2J_{\text{CP}}$ = 6.2 Hz, RuC), 208.92 (t, $^2J_{\text{CP}}$ = 9.0 Hz, CO).

Preparation of a 4:1 Mixture of Ru(BH₄)(CO)[2,6-(CH₂PBu₂)₂C₆H₃] (4a) and RuH(CO)[1-BH₃-2,6-(CH₂PBu₂)₂C₆H₃] (4b). A suspension containing **1** (0.76 g, 1.36 mmol) and [Bu₄N]BH₄ (0.4 g, 1.56 mmol) in Et₂O (10 mL) was stirred for 24 h. The solids were filtered off and washed with 3 × 5 mL of Et₂O. Addition of 10 mL of hexane and cooling (-35 °C) of the solution yielded a yellow crystalline solid (0.28 g). The mother liquor was evaporated, and the residue was washed with 3 × 2 mL of hexane and dried under vacuum. Both isolated fractions were spectroscopically identical. Total yield: 0.44 mg (60%). Anal. Calcd for C₂₅H₄₇BOP₂Ru (537.48): C, 55.87; H, 8.81. Found: C, 55.74; H, 8.92. **Spectroscopic Data for 4a.** IR (Nujol): ν_{BH} 2444, 2335 cm⁻¹, ν_{BHRu} 1939, 1948 cm⁻¹, ν_{CO} 1910 cm⁻¹. ¹H NMR (C₆D₆): δ -5.4 (br, 2H, Ru-H-B), 1.20, 1.29 (vt, $^{\nu}J$ = 6.2, 6.7 Hz; 36H, CH₃), 3.11 (m, overlapped 4H, CH₂), 4.0 (br, 2H, BH₂), 7.00 (s, 3H, C₆H₃). ³¹P{¹H} NMR (C₆D₆): δ 73.9. ¹³C{¹H} NMR (C₆D₆): δ 30.06, 30.34 (vt, $^{\nu}J$ = 1.9, 2.8 Hz, CH₃), 36.55 (vt, $^{\nu}J$ = 6.8 Hz, PCH₂), 36.64 (vt, $^{\nu}J$ = 11 Hz, CH₂), 37.34 (vt, $^{\nu}J$ = 7.5 Hz, PCH₂), 121.80 (vt, $^{\nu}J$ = 7.6 Hz, CH, Ar), 123.53 (s, CH, Ar), 150.01 (vt, $^{\nu}J$ = 6.8 Hz, C, Ar), 164.46 (t, $^2J_{\text{CP}}$ = 2.3 Hz, RuC), 206.83 (t, $^2J_{\text{CP}}$ = 10.1 Hz, CO).

Preparation of RuH(CO)[1-BH₃-2,6-(CH₂PBu₂)₂C₆H₃] (4b). A 1 M solution of BH₃·THF in THF (0.6 g, 0.67 mmol) was added to RuH(CO)(PCP) (0.3 g, 0.57 mmol), and the mixture turned yellow upon stirring with a spatula. Then 3 mL of hexane was added and the solid was filtered, washed with 2 × 3 mL of hexane, and dried in vacuo. Yield: 285 mg (92%). Anal. Calcd for C₂₅H₄₇BOP₂Ru (537.48): C, 55.87; H, 8.81. Found: C, 55.92; H, 8.72. IR (Nujol): ν_{BH} 2436, 2397, 2342 cm⁻¹, ν_{BHRu} and ν_{CO} 1911, 1901 cm⁻¹, ν_{RuH} 2030 cm⁻¹. ¹H NMR (THF-*d*₈): δ -11.07 (t, $^2J_{\text{HP}}$ = 17.0 Hz, 1H, Ru H), -4.03 (br, 1H, Ru-H-B), 1.26, 1.43 (vt, $^{\nu}J$ = 6.5 Hz, 36H, CH₃), 2.5 (br, 2H, BH₂), 2.72 (dvt, $^2J_{\text{HH}}$ = 14.9 Hz, $^{\nu}J$ = 4.0 Hz, 2H, CH₂), 4.04 (dvt, $^{\nu}J$ = 5.6 Hz, 2H, CH₂), 6.82 (d, $^3J_{\text{HH}}$ = 7.3 Hz, 2H, C₆H₃), 7.29 (t, 1H, C₆H₃). ³¹P{¹H} NMR (THF-*d*₈): δ 53.5. ¹³C{¹H} NMR (THF-*d*₈): δ 30.22, 30.31 (vt, $^{\nu}J$ = 2.3, 2.6 Hz,

Table 2. Crystallographic Data for Complexes **3**, **4b**, and **5a,b**

	3	4b	5a,b
formula	C ₂₅ H ₄₄ OP ₂ Ru	C ₂₅ H ₄₇ BOP ₂ Ru	C ₄₈ H ₈₈ N ₂ P ₄ Ru ₂
fw	523.61	537.45	1019.28
cryst syst	triclinic	monoclinic	triclinic
space group	<i>P</i> $\bar{1}$	<i>P</i> 2 ₁	<i>P</i> $\bar{1}$
<i>a</i> , Å	11.8730(18)	10.557(2)	14.348(5)
<i>b</i> , Å	14.030(2)	11.697(2)	14.866(4)
<i>c</i> , Å	16.516(3)	11.281(2)	15.132(4)
α , deg	93.180(3)	90	106.55(2)
β , deg	102.938(3)	95.71(3)	110.39(2)
γ , deg	103.332(3)	90	102.14(3)
<i>V</i> , Å ³	2592.4(7)	1386.1(4)	2722.5(17)
<i>Z</i>	4	2	1
temp, K	110	298	143
abs coeff, mm ⁻¹	0.7	0.7	0.7
total no. of rflns	32331	3677	9931
no. of unique rflns	14434	3497	9517
<i>R</i> , %	5.37	7.66	4.75
<i>R</i> _w , %	12.33	25.97	12.28

^a All data collected with Mo K α radiation (λ = 0.710 69 Å). *R* = $\sum ||F_o| - |F_c|| / \sum |F_o|$; *R*_w = $[\sum (w(F_o^2 - F_c^2)^2) / \sum (w(F_o^2)^2)]^{1/2}$.

CH₃), 33.18 (vt, $^{\nu}J$ = 8.8 Hz, PCH₂), 36.01 (vt, $^{\nu}J$ = 6.1 Hz, PCH₂), 37.57 (vt, $^{\nu}J$ = 10.0 Hz, CH₂), 122.46 (br, line width 100 Hz, BOC), 125.60 (vt, $^{\nu}J$ = 5.9 Hz, CH, Ar), 133.83 (t, $^4J_{\text{CP}}$ = 1.5 Hz, CH, Ar), 168.41 (vt, $^{\nu}J$ = 3.5 Hz, C, Ar), 208.34 (t, $^2J_{\text{CP}}$ = 11.7 Hz, CO).

Preparation of {RuH[2,6-(CH₂PBu₂)₂C₆H₃]}₂(μ -N₂) (5a). Upon stirring, 30 mL of ethanol was added to a mixture of RuHCl[1,3-(CH₂PBu₂)₂C₆H₄] (1.7 g, 3.19 mmol) and [Bu₄N]-BH₄ (0.9 g, 3.50 mmol) in a 100 mL flask under N₂ (ca. 5 mmol). Stirring continued for 18 h. A dark solid precipitated and was isolated by filtration, washed with 4 × 5 mL of ethanol, and dried in vacuo for 2 h. Yield: 1.48 g (91%). Anal. Calcd for C₄₈H₈₈N₂P₄Ru₂ (1019.28): C, 56.56; H, 8.70; N, 2.75. Found: C, 56.40; H, 8.63; N, 2.93. IR (Nujol): ν_{RuH} 2160 cm⁻¹. ¹H NMR (C₆D₆, under vacuum): δ -31.64 (br, line width = 70 Hz, 1H, Ru H), 1.14, 1.17, 1.29, 1.31 (vt, $^{\nu}J$ = 7 Hz; 36H, CH₃), 3.32 (m, overlapped 4H, CH₂), 7.07 (t, $^3J_{\text{HH}}$ = 7.3 Hz, 1H, C₆H₃), 7.21 (d, 2H, C₆H₃). ³¹P{¹H} NMR (C₆D₆): δ 92.30, 93.04 (d, $^2J_{\text{PP}}$ = 259 Hz, doublet of doublets in the hydride-coupled spectrum, $^2J_{\text{PH}}$ = 19 Hz).

RuH(N₂)[2,6-(CH₂PBu₂)₂C₆H₃] (5c). IR (toluene): $\nu_{\text{N=N}}$ 2088 cm⁻¹. ¹H NMR (C₆D₆, under vacuum): δ -29.73 (t, $^2J_{\text{HP}}$ = 18.8 Hz, 1H, Ru H), 1.09, 1.21 (vt, $^{\nu}J$ = 6 Hz, 36H, CH₃), 3.27 (m, overlapped 4H, CH₂), 7.05 (t, $^3J_{\text{HH}}$ = 7.3 Hz, 1H, C₆H₃), 7.17 (d, 2H, C₆H₃). ³¹P{¹H} NMR (C₆D₆): δ 90.77 (s, doublet in the hydride-coupled spectrum). ¹³C{¹H} NMR (C₆D₆): δ 29.42, 30.42 (vt, $^{\nu}J$ = 3 Hz, CH₃), 34.80 (vt, $^{\nu}J$ = 7.8 Hz, PCH₂), 36.99 (vt, $^{\nu}J$ = 5.3 Hz, PCH₂), 37.19 (vt, $^{\nu}J$ = 10.5 Hz, PCH₂), 120.79 (vt, $^{\nu}J$ = 8.6 Hz, CH, Ar), 122.87 (t, $^4J_{\text{CP}}$ = 1 Hz, CH, Ar), 153.91 (vt, $^{\nu}J$ = 11.2 Hz, C, Ar), 182.82 (t, $^2J_{\text{CP}}$ = 5.4 Hz, RuC).

Crystallographic Data for 3, 4b, and 5a,b. ORTEP views of the molecular structures are shown in Figure 1. Selected bond lengths and angles are listed in Table 1. Important details of the data collection and structure refinement are summarized in Table 2. Data reduction and further calculations were performed using the SAINT and SHELXTL-97 program packages.

Structure Determination of 3. Intensities of 32 331 reflections were measured on a Smart 1000 CCD diffractometer (λ (Mo K α) = 0.710 73 Å, ω -scan with 0.5° step and 20 s per frame exposure, $2\theta < 60^\circ$), and 14 434 independent reflections (*R*_{int} = 0.0696) were used in further refinement. The structure was solved by direct methods and refined by the full-matrix least-squares technique against *F*² in the anisotropic

approximation. The hydride was located and refined isotropically. The refinement converged to $wR2 = 0.1233$ and $GOF = 0.995$ for all independent reflections ($R1 = 0.0537$ was calculated against F for 7783 observed reflections with $I > 2\sigma(I)$).

Crystallographic Data for 4b. Experimental data were collected at room temperature with an Enraf-Nonius CAD4 four-circle automatic diffractometer (Mo $K\alpha$ monochromated radiation, $\theta/2\theta$ scan, $2\theta \leq 56^\circ$). The structure was solved by direct methods and refined by the full-matrix least-squares technique using anisotropic approximation for all non-hydrogen atoms. The absolute structure was determined by the refinement of the Flack parameter ($x = 0.1(2)$). Hydrogen atoms bonded to ruthenium and boron atoms were located and refined isotropically; all other H atoms were placed in calculated positions and refined in the riding model approximation. The final values of $R1 = 0.077$ (on F for 2843 observed reflections with $I > 2\sigma(I)$) and $wR2 = 0.260$ (on F^2 for all 3497 reflections).

Crystallographic Data for 5a,b. Intensities of 9931 reflections were measured on a Syntex $P2_1$ diffractometer ($\lambda(\text{Mo } K\alpha) = 0.71073 \text{ \AA}$, $\theta/2\theta$ scan, $2\theta < 50^\circ$), and 9517 independent reflections ($R_{\text{int}} = 0.0279$) were used in further refinement. The structure was solved by direct methods and

refined by the full-matrix least-squares technique against F^2 in the anisotropic approximation with the exception of the disordered N_2 ligand with low occupancy, which according to the refinement was 0.2 (for $N(3)\equiv N(4)$), 0.1 (for $N(5)\equiv N(6)$), and 0.3 (for $N(7)\equiv N(8)$). The hydrides were located and refined isotropically. Each hydride ligand was found disordered in two positions with equal occupancies. Figure 1 shows only one hydride and one N_2 ligand in each ruthenium fragment. The refinement converged to $wR2 = 0.1228$ and $GOF = 1.094$ for all independent reflections ($R1 = 0.0475$ was calculated against F for 8309 observed reflections with $I > 2\sigma(I)$).

Acknowledgment. This work was supported by Wilfrid Laurier University and grants from the Natural Sciences and Engineering Research Council (NSERC) of Canada and Petro-Canada.

Supporting Information Available: Tables of atomic coordinates, bond lengths, bond angles, and anisotropic thermal parameters for **3**, **4b**, and **5a,b**. This material is available free of charge via the Internet at <http://pubs.acs.org>.

OM0003842